coatings

MDPI

Article

Impact of Hard and Soft Reinforcements on the Microstructure, Mechanical, and Physical Properties of the Surface Composite Matrix Manufactured by Friction Stir Processing

Waheed Sami Abushanab [1], Essam B. Moustafa [2], Emad Ismat Ghandourah [3], Hossameldin Hussein [4], Mohammed A. Taha [5] and Ahmed O. Mosleh [6,*]

1 Marine Engineering Department, Faculty of Maritime Studies and Marine Engineering, King Abdulaziz University, Jeddah 21589, Saudi Arabia
2 Mechanical Engineering Department, Faculty of Engineering, King Abdulaziz University, Jeddah 80204, Saudi Arabia
3 Department of Nuclear Engineering, Faculty of Engineering, King Abdulaziz University, Jeddah 21589, Saudi Arabia
4 Mechanical and Mechatronics Engineering Department, Higher Technological Institute, Tenth of Ramadan City 44637, Egypt
5 Solid State Physics Department, National Research Centre, El Buhouth St., Dokki, Giza 12622, Egypt
6 Mechanical Engineering Department, Faculty of Engineering at Shoubra, Benha University, Cairo 11629, Egypt
* Correspondence: ahmed.omar@feng.bu.edu.eg

Abstract: This work studies the effect of incorporating a mix of reinforcement particles of a hard and soft nature on the microstructure and mechanical and physical properties of a high-strength aluminum alloy, AA7075. A friction stir processing technique was used for compositing the surface of this alloy. The vanadium carbide (VC) was selected to be the hard reinforcement, while the boron nitride (BN) and graphene nanoplates (GNPs) were chosen as soft reinforcements. Mono VC, hybrid reinforcements combined of 50 vol.% VC and 50 vol.% BN, and triple reinforcements combined of 33.4 vol.% VC, 33.3 vol.% BN, and 33.3 vol.% GNPs were used for producing the composites. Intensive grain refinement was observed, 930%, in the composite with triple reinforcements. The microhardness and the ultimate compressive strength were improved and reached b0, 29%, respectively, in composites that contained GNPs. The thermal properties were significantly improved, and the coefficients of thermal expansion (CTE) and thermal conductivity decreased to 88% and 15%, respectively. The composite's electrical conductivity was decreased by 58% with triple reinforcements.

Keywords: surface composite; reinforcement particles; aluminium alloys; thermal conductivity; microstructure

check for updates

Citation: Abushanab, W.S.; Moustafa, E.B.; Ghandourah, E.I.; Hussein, H.; Taha, M.A.; Mosleh, A.O. Impact of Hard and Soft Reinforcements on the Microstructure, Mechanical, and Physical Properties of the Surface Composite Matrix Manufactured by Friction Stir Processing. *Coatings* **2023**, *13*, 284. https://doi.org/10.3390/coatings13020284

Academic Editor: Alina Vladescu

Received: 13 January 2023
Revised: 22 January 2023
Accepted: 25 January 2023
Published: 26 January 2023

Copyright: © 2023 by the authors. Licensee MDPI, Basel, Switzerland. This article is an open access article distributed under the terms and conditions of the Creative Commons Attribution (CC BY) license (https://creativecommons.org/licenses/by/4.0/).

1. Introduction

Nowadays, weight reduction is in high demand in the automotive and aerospace industries; therefore, it is important to manufacture products from lightweight materials. Aluminum alloys and other lightweight metals should be used in place of heavier materials, leading to reduced energy and fuel consumption and, thus, reduced emission of CO_2 [1,2]. However, aluminum alloys are not stiff or strong enough for many uses, so they need to be strengthened [3]. One of the feasible approaches for strengthening aluminum alloys is producing aluminum metal matrix composites (AMMCs). Through the process of incorporating one or more reinforcing particles with a hard nature, the AMMCs are manufactured. AMMCs have attracted considerable interest in modern engineering applications, such as military and civil defense, automotive, and aerospace industries. Particle-reinforced metal matrix composites' physical and mechanical characteristics strongly depend on the characteristics of the reinforcement particles, taking into consideration the matrix's characteristics, the reinforcement materials, and the manufacturing processes [4,5]. Friction

stir processing (FSP) is considered a valuable approach for producing AMMCs with an inexpensive ultrafine-grained structure containing a uniform distribution of heavy hard-reinforced particles. Adding reinforcing particles makes the aluminum alloy's surface composite harder; several authors have noted that the reinforcement impacts how the composite surface resists scratches [6–8].

Aluminum alloys, particularly heat-treatable AA7075, have been the subject of extensive research to make AMMCs [9,10]. Al7075 is preferred in the aerospace and automotive industries because of its extremely high tensile strength/hardness-to-weight ratio [11]. According to Doel and Bowen [12], AA7075 reinforced with 5 and 13 μm SiC particles has higher tensile strength and lower ductility than unreinforced material. Baradeswaran and Perumal [13] improved the mechanical properties, tribological behavior, wear resistance, and coefficient of friction of AA7075 alloy by incorporating B4C particles by stir casting. Incorporating heavy hard particles in the AMMCs was successfully performed by several methods, such as conventional stirring casting. The heavy parts' specific density helps enhance the distribution of these particles inside the AMMCs [8,14,15]. Incorporating lightweight, soft reinforcements with nanoscale, such as boron nitride (BN) and graphene nanoplates (GNPs) within AMMCs, is a research challenge that needs extensive work [16]. Although there are benefits of such reinforcements, the manufacturing of composites with non-uniform dispersion of these reinforcements limits their applications. BN and GNPs are strong lubricant reinforcements that improve the mechanical and tribological properties of the composites [17,18]. FSP effectively solved this challenge by producing composites with uniform distribution of heavy hard and light soft reinforcements [19–22].

This paper aims to combine heavy-hard particles such as VC with light-soft reinforcements such as BN and GNPs to manufacture a surface composite with outstanding properties. The aim of using lightweight-soft materials is to decrease the final weight of the manufactured composites while maintaining or even improving the mechanical properties of the AA7075 aluminum alloy. Many properties of the alloy were research targets in this study, including increasing the mechanical properties, decreasing the thermal expansion, decreasing the thermal conductivity, and improving the structure features, grain refining, and uniform distribution.

2. Materials and Experiments

In this study, rolled plates of commercial AA7075 aluminum alloy with the chemical composition specified in Table 1 were chosen to make the surface composite. The reinforcement materials were selected to have soft and hard natures. Thus, VC was selected for the hard particles, while BN and GNPs were selected as soft nature reinforcements. The specifications of the used reinforcements are listed in Table 2.

Table 1. Chemical composition of the used aluminum metal matrix alloy, AA7075 (wt%).

Zn	Mg	Cu	Cr	Fe	Si	Mn	Balance
5.7	2.3	1.4	0.18	0.35	0.2	0.2	Al

Table 2. Specifications of the used reinforcements.

Reinforcement	Dimensions	Purity (%) *	Density (g/cm^3)
VC	Diameter = 300:550 nm	>99	5.77
BN	Diameter = 100 ± 10 nm	99	2.1
GNPs	Thickness = 7 ± 0.6 nm Wide = 5 ± 0.5 μm	>99	2.2

* According to the supplier; Nanoshel-UK-Ltd company (Congleton, UK).

For surface composite manufacturing, the AA7075 plates were prepared by making hole patterns on the surface with dimensions illustrated in Figure 1a; the reinforcements

filled these holes. This work manufactured three different surface composites: (1) surface composite reinforced with mono-hard reinforcement particles, VC; (2) hybrid surface composited with 50 vol.% VC and 50 vol.% BN; (3) surface composite with triple reinforcements 33.4 vol.% VC, 33.3 vol.% BN, and 33.3 vol,% GNPs. Friction stir processing was performed along the reinforcements-filled holes by a triangle pin tool with dimensions shown in Figure 1b. The processing parameters were: 1080 rpm, 30 mm/min, and tilt angle 2°, as the optimum FSP processing parameters for the investigated alloy. After the FSP, the samples for characterizations were cut, as shown in Figure 1c. All samples for characterizations, microstructure analysis, and mechanical and physical properties characterizations were cut from the processed zone to ensure characterizing the manufactured composite parts only. Thus, before the cutting process, the lower and upper unprocessed layers were surface milled, leaving the composite parts only, and then the samples were cut along the manufactured composites parts from the center.

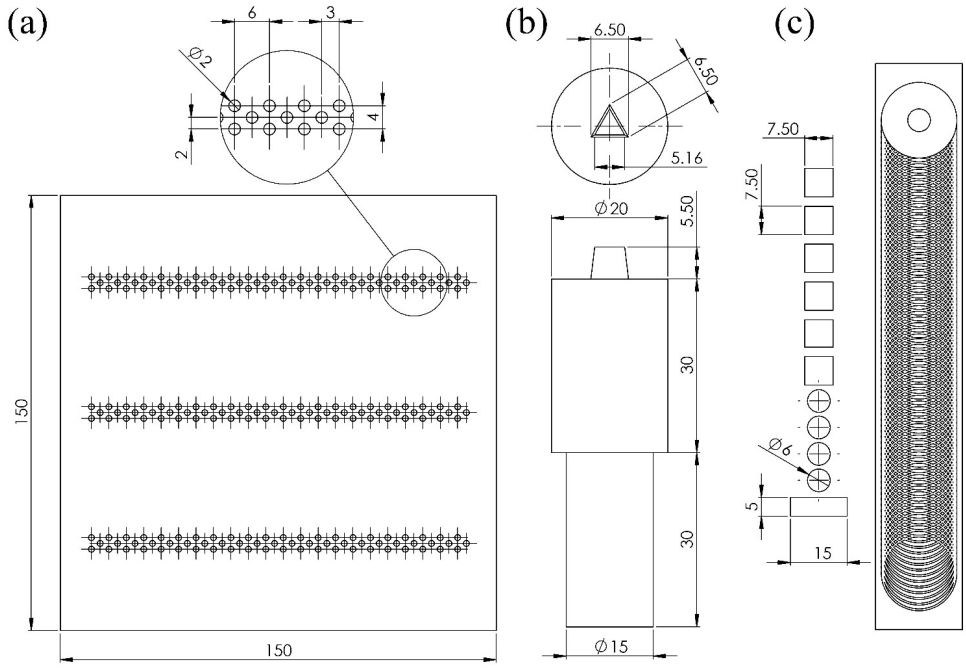


Figure 1. The dimensions of (**a**) holes patterns, (**b**) FS processing tool, and (**c**) samples for characterization and their places. All dimensions in mm. (ø is the diameter)

For microstructure observation, according to the ASTM E3-11 Standard Guide [23], the samples were mechanically ground using SiC polishing papers starting from 180 grit followed by 320, 600, 800, 1200, 2400, then 4000 grit in the water as a lubricant media with a applied force of 20 N and a rotating speed of 200 rpm for several minutes. The ground samples were polished on emery cloth into alumina suspension with 0.1µm with an applied force of 15 N and a rotating speed of 100 rpm. Before microscopy characterizations, the samples were etched using metallurgical standard agents, Kellers. Olympus Light optical microscopy (BX51, Olympus Optical, Tokyo, Japan) and Tescan-VEGA3 scanning electron microscopy (SEM, Tescan Vega3 SB, Brno, Czech Republic)) were used for microstructure characterizations. SEM imaging was carried out at working distances of 10–15 mm using an accelerating voltage of 20 kV in secondary-electron (SE) mode. Using the linear intercept method according to ASTM E112-10 [24], the grain size was measured, and then the distributions of the grain size were constructed.

Mechanical properties were characterized using microhardness and compression tests. The Vickers microhardness (Zwick/Roell, Kennesaw, GA, USA) was performed according to the ASTM ASTM: B933-09 with a load of 1.961 N for 10 s. The compression test was

carried out according to ASTM E9 for three samples with dimensions of ø6 mm and a height of 9 mm, and then the average of the recorded data was plotted.

Physical properties such as thermal analysis and electrical conductivity were evaluated. The electrical conductivity of the base metal and manufactured composites was measured at room temperature, via the Keithley 6517B system based on Ref [25], and calculated using Equation (1).

$$\text{Electrical Conductivity} = \frac{h}{RA} \quad (1)$$

where, h, A, and R are the sample diameter, surface area, and the electrical resistance, respectively.

The thermal expansion was measured at a temperature range of 25–400 °C via a thermal dilatometer (NETZSCH DIL 402 PC, Selb, Germany) with a heating rate of 5 °C/min [26]. The thermal conductivity measurement procedures were explained in detail in ref. [27].

3. Results and Discussion

3.1. Microstructure Analysis

Figure 2 shows the optical microscopy microstructure of the as-rolled plates and the manufactured composites. The captured photos of the manufactured composites were in the center of the processed zone. The base material proceeded as a rolled sheet; thus, the deformed grains were noted in the rolling direction (Figure 2a). The average grain size of the base metal (BM) was 180 ± 20µm with an aspect ratio (light/thickness) of 2.5. The friction stir processing resulted in a significant refinement in the stirred or processed zone (PZ). In the PZ, the generated heat from the friction between the rotating tool and the base metal was enough for full recrystallization resulting in equiaxed grains for all the manufactured composites (Figure 2b–d). The distributions of the grains in the PZ of the manufactured composites are demonstrated in Figure 3. Theoretically, processing at the same condition for the same base metal should result in the same refinement action. The different reinforcements' presence particularly alters the manufactured composite's refinement action. The presence of the reinforcements restricted grain growth after the recrystallization during the FSP. The restriction was different for each composite depending on the existing reinforcement. For the composite with mono-reinforcement particles (VC), the average grain size was 23.4 ± 0.6µm (Figure 3a). Adding soft-nature reinforcement BN to form a hybrid surface composite resulted in a slight improvement in grain size, 22.6 ± 0.6µm (Figure 3b). The refinement of the manufactured composite with triple reinforcements (VC + BN + GNPs) was greater than that of other composites; it was 18.5 ± 0.5µm (Figure 3c). The improvement in the refining effect in the composite containing GNPs may be attributed to the nature and the morphology of the used GNP. GNPs have a large contact area that can surround the grains after recrystallization, eliminating grain growth. From the distribution curves, all manufactured composites exhibited normal distribution around the mean (Figure 3). In the case of the composite with triple reinforcements, the distribution was narrow around the mean, which revealed greater uniformity in grain size than the other composites. The standard deviations of the manufactured composites; AA7075/VC, AA7075/VC + BN, and AA7075/CV + BN + GNPs were 6.2, 6.3, and 4.7µm, respectively.

Figure 4 demonstrates the SEM micrographs of the manufactured composites. The main aim of performing the SEM characterizations is to show the distribution of the reinforcements and their presence. AA7075 is a high-strength aluminum alloy; thus, processing this alloy with a guarantee of uniform distribution of the reinforcers is difficult, especially when incorporating hybrid and triple reinforcements with different natures. The attached SEM micrographs prove the successfulness of producing the surface composites with uniform distribution of the reinforcements. Agglomeration of particles was not observed in the nonreinforcement composite due to the uniform VC particle size (Figure 4a). A small area with agglomeration of particles was observed in the hybrid-reinforcement composite (VC + BN), which can be attributed to the difference in the grain size of particles and the soft nature of the BN (Figure 4b). Agglomeration of the reinforcement was not

observed in the composite with triple reinforcements. The lack of agglomeration should improve the properties of the manufactured composites.

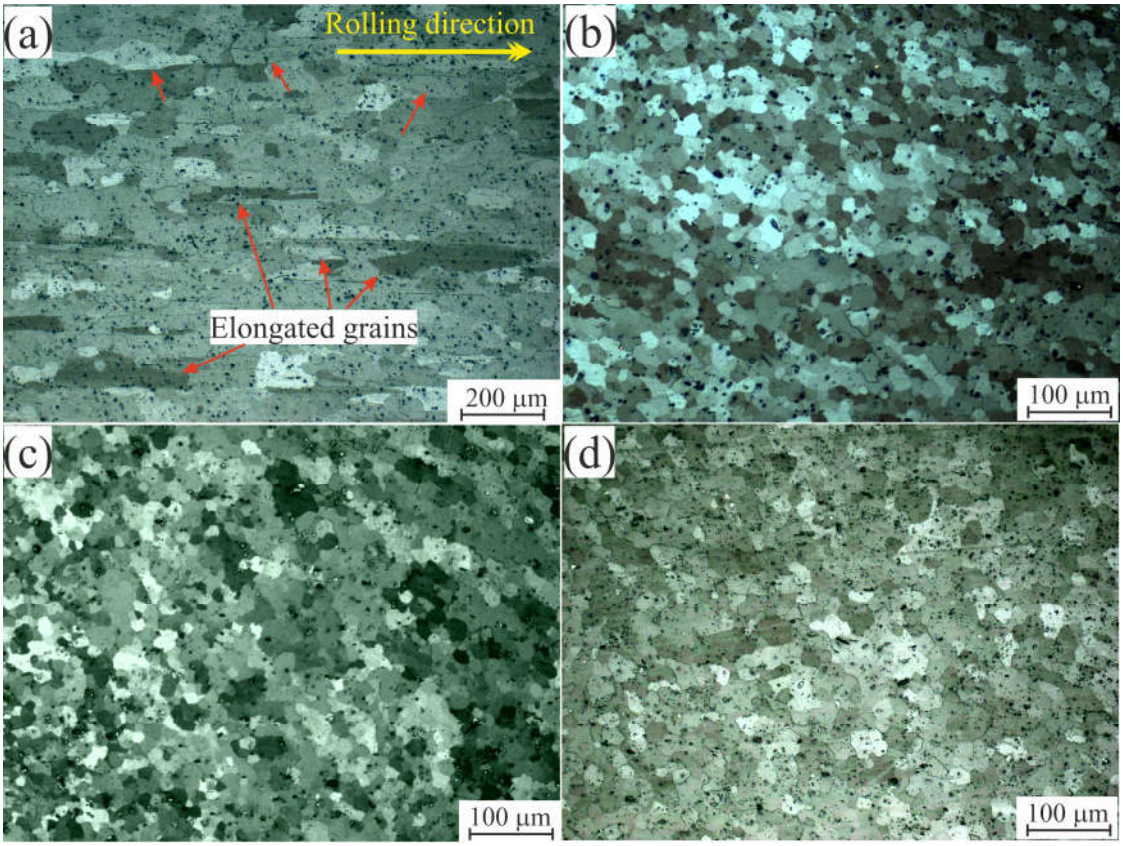


Figure 2. Optical microscope micrographs of (**a**) as-rolled plates (base metal), (**b**) composite with mono-reinforcement (VC), (**c**) composite with the hybrid-reinforcements (VC + BN), and (**d**) composites with triple-reinforcements (VC + BN + GNPs).

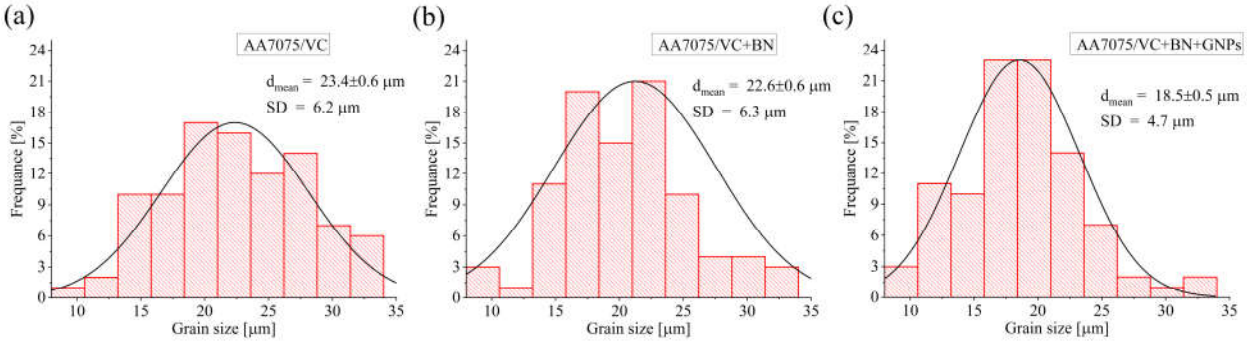


Figure 3. Grain size distributions of the manufactured composites reinforced with (**a**) mono-reinforcement (VC), (**b**) hybrid-reinforcements (VC + BN), and (**c**) triple-reinforcements (VC + BN + GNPs).

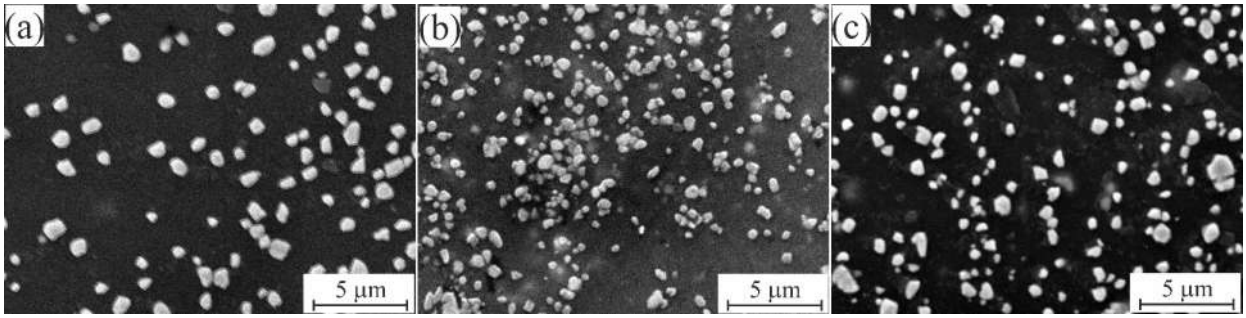


Figure 4. SEM micrographs of the manufactured composites reinforced with: (**a**) mono-reinforcement (VC), (**b**) hybrid-reinforcements (VC + BN), and (**c**) triple-reinforcements (VC + BN + GNPs).

3.2. Mechanical Properties Analysis

The effect of incorporating mono, hybrid, and triple reinforcements on microhardness and ultimate compressive strength of the AA7075 alloy-based composites manufactured by FSP is shown in Figure 5. The average value of the microhardness of base metal, as processed AA7075 plates, in the present work was 115 ± 5 HV. Compositing the AA7075 plates with mono-reinforcement (VC), hybrid reinforcements (VC + BN), and triple reinforcements (VC + BN + GNPs) increased the microhardness to 137 ± 7, 164 ± 7 and 183 ± 6 HV, respectively (Figure 5a). The ultimate compressive strength of the base metal alloy was 411 ± 10 MPa and this was increased by adding mono/hybrid/triple reinforcements, givint levels of 467 ± 9, 492 ± 12, and 519 ± 10 MPa, respectively (Figure 5b).

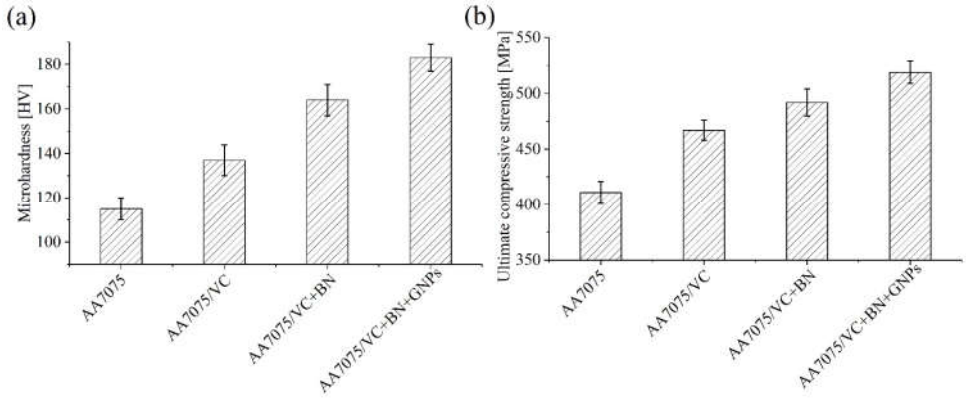


Figure 5. Mechanical properties of the manufactured composites. (**a**) Microhardness and (**b**) ultimate compressive strength.

The specific improvement in the microhardness and ultimate compressive strength of the AA7075 alloy matrix after incorporating mono-reinforcement (VC), hybrid reinforcements (VC + BN), and triple reinforcements (VC + BN + GNPs) can be attributed to three factors. Firstly, according to the rule of mixtures, adding hard ceramic particles with uniform distribution can increase the microhardness of composites (Orowan strengthening mechanism), as in Equation (2) [28].

$$H_C = H_M F_M + \sum H_R F_R \quad (2)$$

where *Hc* stands for the microhardness of the mono/hybrid/triple reinforcements composite, H_M and H_R stand for the microhardness of the AA7075 and the reinforcements, respectively, and F_M and F_R represent the amount of the matrix and the reinforcing particles (vol.%), respectively. Secondly, according to the Hall–Petch relation (Equation (3)), grain size has an influence on the mechanical characteristics of Al alloys. Due to the grain

refinement in the PZ, which is less than that of the AA7075 base matrix, the grain boundary strengthening increased [29].

$$\sigma_{GB} = \sigma_0 + K\frac{1}{\sqrt{d}} \quad (3)$$

where σ_{GB} is the grain boundary strengthening, σ_0 and K are constants and can be determined experimentally, and d is the average grain size. Finally, according to the Orowan mechanism, the contact between the dislocations and the VC, BN and GNPs reinforcements increased the strength of the manufactured composite samples. As a result of the matrix's scattering of reinforcement particles, the dislocations' interactions with them result in the formation of dislocation loops. As a result of the reinforcement particles scattered into the AA 7075 matrix, dislocation interactions with them lead to dislocation rings forming [30].

3.3. Physical Characterizations

3.3.1. Thermal Analysis

Figure 6a shows the fractional change in the length ($\Delta L/L_0$, where ΔL is the change in the length and L_0 is the original length of the tested sample) of the base metal AA7075 and the manufactured composite with different reinforcements in a temperature range of 25–400 °C. It is clear from the figure that increasing the temperature has a significant positive effect (high line inclination) on the change of the length of AA7075 alloy, while incorporating reinforcements, whether mono, hybrid or triple, has a slight effect (low line inclination). For example, at 100 °C, the $\Delta L/L_0$ values of the composites with VC, VC + BN, and VC + BN + GNPs are 2.27×10^{-3}, 1.88×10^{-3}, 1.70×10^{-3} and 1.24×10^{-3}, respectively. For the same samples, the values of $\Delta L/L_0$ are 11.00×10^{-3}, 9.37×10^{-3}, 8.22×10^{-3}, and 5.88×10^{-3}, respectively, when the temperature is increased to 400 °C. This behavior, due to the kinetic energy of AA7075 atoms, causes it to expand. When the AA7075 alloy is heated, the increase in energy causes the atoms and molecules to move faster and take up more space, causing expansion. Adding reinforcement ceramics may impede the movement of the atoms and thus reduce the expansion process.

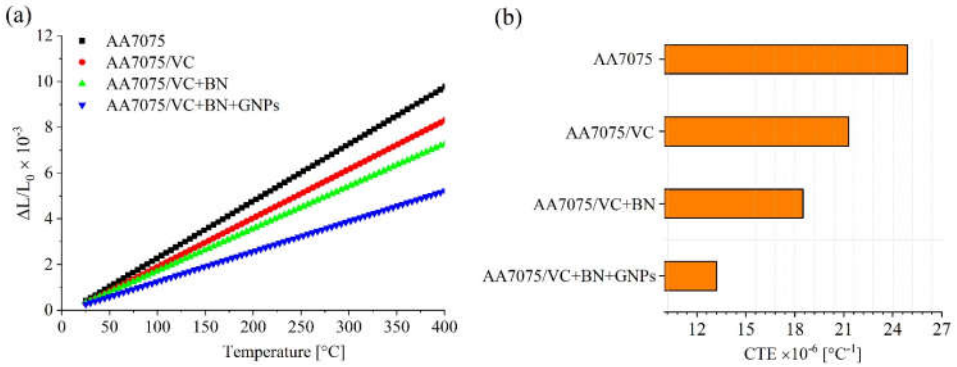


Figure 6. (**a**) Fractional change in the length ($\Delta L/L_0$) and (**b**) the coefficient of thermal expansion, CTE, for the base alloy AA7075 and the manufactured composites.

For linear expansion, the coefficient of thermal expansion, CTE (μm/m °C) = $(1/L_0) \times (\Delta L/\Delta T)$, where ΔT is the temperature change calculated by the mathematical differentiation of the plotted lines in Figure 6a. The CTE of base alloy and the manufactured composites reinforced with mono, hybrid, and triple reinforcements is demonstrated in Figure 6b. The value of CTE of AA7075 is 24.9×10^{-6} °C^{-1} which decreases to 21. 3×10^{-6}, 18.5×10^{-6} and 13.2×10^{-6} °C^{-1} after incorporating VC, VC + BN and VC + BN-GNPs reinforcements. It is worth mentioning that the lowered CTE value of all composites may be due to the high thermal stability of reinforcements VC, BN, and GNPs. The VC, BN, and GNPs exhibit theoretical CTE of 7.2×10^{-6}, $11.6 \times 10^{-6,}$ and 3.2×10^{-6} °C^{-1}, respectively, which are lower than that of AA7075 alloy (≈25.1×10^{-6} °C^{-1}) [26,31].

Figure 7 shows the thermal conductivity of the AA7075 matrix alloy and the manufactured composites. The figure reveals that the thermal conductivity of the AA7075/VC composite is 133.1 W/mK, which shows a decrease of about 6.7% compared with the thermal conductivity of AA775 base alloy (142.5 W/mK). It may also be noted that the thermal conductivity of the AA7075/VC + BN hybrid composite continued to decrease as it recorded 121.2 W/mK, which decreased by about 15 and 9.1% compared to the AA7075 alloy and the composite with mono reinforcement (VC), respectively. Surprisingly, the thermal conductivity of AA7075/VC + BN + GNPs composites was 130.1 W/mK, which shows a decrease of 8.9% compared to the base alloy [32,33]. It is worth noting that this remarkable change in the conductivity value of the AA7075 alloy, whether by adding mono or hybrid, or triple reinforcements, is due to the ability of these reinforcements in thermal conductivity compared to the base aluminum alloy. It is known that GNPs have very heavy thermal conductivity, which is about ~4000 W/mK [34]; hence, they have increased the thermal conductivity of the composite with triple reinforcement, unlike both BN and VC, which have a negative effect on the conductivity because their thermal conductivity is about 7.1 and 33 W/mK, respectively.

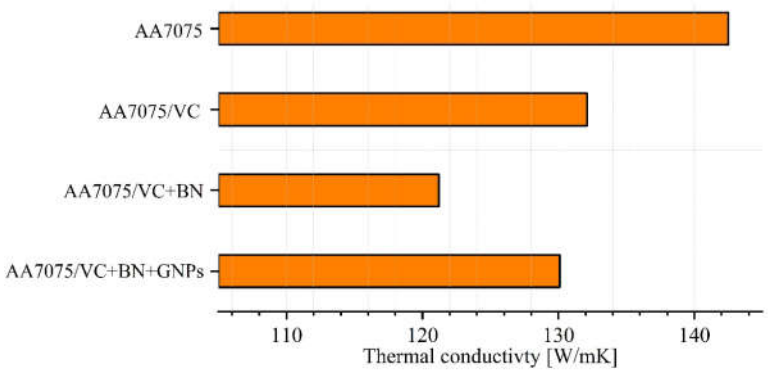


Figure 7. The thermal conductivity of the base alloy AA7075 and the manufactured composites.

3.3.2. Electrical Conductivity

Figure 8 demonstrates the electrical conductivity of the AA7075 alloy matrix and the manufactured composites. It appears from the figure that the electrical conductivity of AA7075 alloy was decreased when adding mono, hybrid, and triple reinforcements. The electrical conductivity of the AA7075 base alloy was recorded as 1.55×10^7 S/m. The electrical conductivity of the composites reinforced with mono-reinforcement (VC), composites reinforced with hybrid-reinforcements (VC + BN), and composites reinforced with triple-reinforcements (VC + BN + GNPs) recorded 1.36×10^7, 1.05×10^7 and 9.79×10^6 S/m, respectively. The lower electrical conductivity of the manufactured composites compared to the base is due to the conduction process that depends on the ease of movement of free electrons within AA7075 alloy. Therefore, when reinforcements are added to the AA7075 alloy, it creates a barrier against the movement of free electrons and thus provides lower electrical conductivity. Moreover, the difference in the conductivity of the composites also depends on the role of ceramics reinforcement in the electrical conductivity; the addition of GNPs has a small effect on the conductivity because it acts as an insulator [20,31]. In the case of the other reinforcements, as the electrical conductivity of BN and VC are about 1×10^{-8} and 1.6×10^4 s/m, respectively, their effect is more than that of GNPs on lowering electrical conductivity [35].

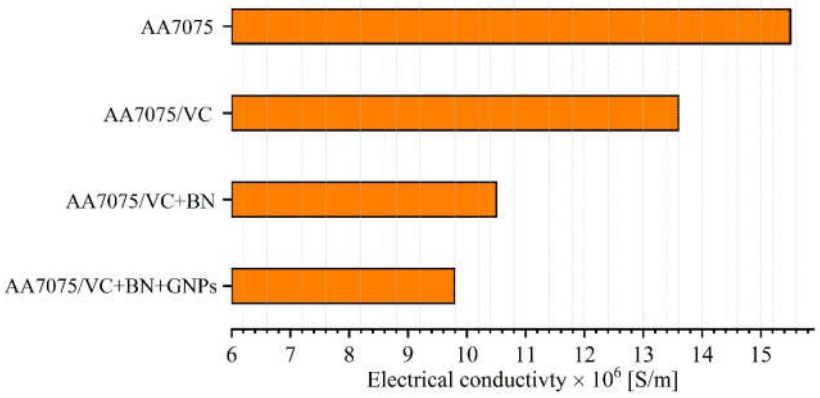


Figure 8. The electrical conductivity of the base alloy AA7075 and the manufactured composites.

Table 3 summarizes the overall improvement achieved in the manufactured composites with respect to the base alloy. As concluded in Table 3, an intensive refinement in the processed zone was observed in all composites and was the maximum in the composite with triple reinforcements. The presence of the soft nature BN and GNPs played a great role in increasing the refinement, and they worked as grain growth barriers. In addition, the mixture of the hard and soft nature reinforcements helped increase the investigated alloy's mechanical properties, hardness, and ultimate compressive strength. GNPs exhibit high thermal conductivity ~4000 W/mK [34], while BN exhibits lower thermal conductivity, 65 W/mK [36], and this is reflected in the measured thermal conductivity of the manufactured composites. The composite with hybrid reinforcements demonstrated a 15% decrease in thermal conductivity, while the composite with triple reinforcements exhibited a decrease of 8.9%. The GNPs significantly decreased the CTE of the manufactured composite due to high thermal stability. The electrical conductivity of the manufactured composites decreased gradually when mono, hybrid and triple reinforcements were used. The maximum decrease was recorded to the composite with triple reinforcements.

Table 3. The overall improvement in the grain size, mechanical, physical, and service properties. All values in % and with respect to the AA7075 base metal.

Property/Composite	AA7075/VC	AA7075/VC + BN	AA7075/VC + BN+GNPs
Grain refining (decreased)	720	740	930
Microhardness (increased)	20	43	60
Ultimate compressive strength (increased)	14	21	29
CTE (decreased)	17	35	88
Thermal conductivity (decreased)	6.7	15	8.9
Electrical conductivity (decreased)	14	48	58

4. Conclusions

In the current study, AA7075 metal matrix surface composites were successfully produced by the friction stir processing (FSP) approach, which was reinforced with different morphology and with hard and soft particle reinforcements. Mono VC hard particles, hybrid reinforcements combining hard and soft particles (50 vol.% VC + 50 vol.% BN), and triple reinforcements combining 33.4 vol.% VC + 33.3 vol.% BN + 33.3 vol.% GNPs were used for producing the surface composites. The microstructure, mechanical, and physical

properties of the manufactured composites were evaluated, and the following conclusions were reached:

- Significant grain refining was achieved in the stirred zone for all composites. The composite containing the GNPs exhibited the best refinement action compared to other reinforcements. The GNPs morphology (large surface area) helped restrict grain growth after the recrystallization during the FSP processing.
- The hardness and the ultimate compressive strength were improved significantly in the processed zone for all manufactured composites. The main reasons for this improvement were the presence of the reinforcements (dispersion strengthening) and the refining of grains (activated the grain boundary strengthening). The best improvement was recorded for the composite with GNPs. The large surface area of the GNPs could increase the adhesion between the matrix and the GNPs.
- The thermal expansion, thermal conductivity, and electrical conductivity were decreased in the manufactured composites, which was attributed to the reinforcements' nature. The produced composites demonstrated thermal stability in their dimensions at the studied temperature range. The lowest thermal conductivity was observed in the composite reinforced with VC and BN.

Author Contributions: Conceptualization, M.A.T.; Methodology, E.B.M., M.A.T. and A.O.M.; Software, A.O.M.; Validation, E.B.M.; Formal analysis, W.S.A., H.H., M.A.T. and A.O.M.; Investigation, E.I.G. and H.H.; Resources, W.S.A. and E.I.G.; Data curation, E.I.G.; Writing—original draft, E.B.M. and M.A.T.; Writing—review & editing, A.O.M.; Supervision, A.O.M.; Funding acquisition, W.S.A. and E.B.M. All authors have read and agreed to the published version of the manuscript.

Funding: This project was funded by the deanship of scientific research (DSR) at King Abdulaziz University, Jeddah, under Grant No. (RG-1-150-43).

Institutional Review Board Statement: Not applicable.

Informed Consent Statement: Not applicable.

Data Availability Statement: Not applicable.

Acknowledgments: This project was funded by the deanship of scientific research (DSR) at King Abdulaziz University, Jeddah, under grant No. (RG-1-150-43). The authors, therefore, gratefully acknowledge technical and financial support from DSR.

Conflicts of Interest: The authors declare no conflict of interest.

References

1. Joost, W.J. Reducing Vehicle Weight and Improving U.S. Energy Efficiency Using Integrated Computational Materials Engineering. *JOM* **2012**, *64*, 1032–1038. [CrossRef]
2. Del Pero, F.; Delogu, M.; Pierini, M. The effect of lightweighting in automotive LCA perspective: Estimation of mass-induced fuel consumption reduction for gasoline turbocharged vehicles. *J. Clean. Prod.* **2017**, *154*, 566–577. [CrossRef]
3. Mishra, R.; Ma, Z.; Charit, I. Friction stir processing: A novel technique for fabrication of surface composite. *Mater. Sci. Eng. A* **2003**, *341*, 307–310. [CrossRef]
4. Jalilvand, M.M.; Mazaheri, Y. Effect of mono and hybrid ceramic reinforcement particles on the tribological behavior of the AZ31 matrix surface composites developed by friction stir processing. *Ceram. Int.* **2020**, *46*, 20345–20356. [CrossRef]
5. García-Vázquez, F.; Vargas-Arista, B.; Muñiz, R.; Ortiz, J.C.; García, H.H.; Acevedo, J. The Role of Friction Stir Processing (FSP) Parameters on TiC Reinforced Surface Al7075-T651 Aluminum Alloy. *Soldag. Inspeção* **2016**, *21*, 508–516. [CrossRef]
6. Moustafa, E.B.; Melaibari, A.; Alsoruji, G.; Khalil, A.M.; Mosleh, A.O. Tribological and mechanical characteristics of AA5083 alloy reinforced by hybridising heavy ceramic particles Ta2C & VC with light GNP and Al2O3 nanoparticles. *Ceram. Int.* **2022**, *48*, 4710–4721. [CrossRef]
7. Jain, V.K.; Yadav, M.K.; Siddiquee, A.N.; Khan, Z.A. Fabrication of surface composites on different aluminium alloys via friction stir process-A review report. *Aust. J. Mech. Eng.* **2022**, 1–24. [CrossRef]
8. Imran, M.; Khan, A.R.A. Characterization of Al-7075 metal matrix composites: A review. *J. Mater. Res. Technol.* **2019**, *8*, 3347–3356. [CrossRef]
9. Sambathkumar, M.; Navaneethakrishnan, P.; Ponappa, K.; Sasikumar, K.S.K. Mechanical and Corrosion Behavior of Al7075 (Hybrid) Metal Matrix Composites by Two Step Stir Casting Process. *Lat. Am. J. Solids Struct.* **2017**, *14*, 243–255. [CrossRef]

10. Arun Kumar, S.; Hari Vignesh, J.; Paul Joshua, S. Investigating the effect of porosity on aluminium 7075 alloy reinforced with silicon nitride (Si3N4) metal matrix composites through STIR casting process. *Mater. Today Proc.* **2021**, *39*, 414–419. [CrossRef]
11. Kumar, G.V.; Rao, C.S.P.; Selvaraj, N.; Bhagyashekar, M.S. Studies on Al6061-SiC and Al7075-Al 2 O 3 metal matrix composites. *J. Min. Mater. Charact. Eng.* **2010**, *9*, 43.
12. Doel, T.J.A.; Bowen, P. Tensile properties of particulate-reinforced metal matrix composites. *Compos. Part A Appl. Sci. Manuf.* **1996**, *27*, 655–665. [CrossRef]
13. Baradeswaran, A.; Elaya Perumal, A. Influence of B4C on the tribological and mechanical properties of Al 7075–B4C composites. *Compos. Part B Eng.* **2013**, *54*, 146–152. [CrossRef]
14. Sahu, M.K.; Sahu, R.K. Synthesis, microstructure and hardness of Al 7075/B4C/Fly-ash composite using stir casting method. *Mater. Today Proc.* **2020**, *27*, 2401–2406. [CrossRef]
15. Suresh, S.; Gowd, G.H.; Deva Kumar, M.L.S. Tribological Behavior of Al 7075/SiC Metal Matrix Nano-composite by Stir Casting Method. *J. Inst. Eng. Ser. D* **2019**, *100*, 97–103. [CrossRef]
16. Saboori, A.; Moheimani, S.; Dadkhah, M.; Pavese, M.; Badini, C.; Fino, P. An Overview of Key Challenges in the Fabrication of Metal Matrix Nanocomposites Reinforced by Graphene Nanoplatelets. *Metals* **2018**, *8*, 172. [CrossRef]
17. Moustafa, E.B.; Melaibari, A.; Basha, M. Wear and microhardness behaviors of AA7075/SiC-BN hybrid nanocomposite surfaces fabricated by friction stir processing. *Ceram. Int.* **2020**, *46*, 16938–16943. [CrossRef]
18. Mehta, K.M.; Badheka, V.J. Wear behavior of boron-carbide reinforced aluminum surface composites fabricated by Friction Stir Processing. *Wear* **2019**, *426*, 975–980. [CrossRef]
19. Khoshaim, A.B.; Moustafa, E.B.; Alazwari, M.A.; Taha, M.A. An Investigation of the Mechanical, Thermal and Electrical Properties of an AA7075 Alloy Reinforced with Hybrid Ceramic Nanoparticles Using Friction Stir Processing. *Metals* **2023**, *13*, 124. [CrossRef]
20. Moustafa, E.B.; Mikhaylovskaya, A.V.; Taha, M.A.; Mosleh, A.O. Improvement of the microstructure and mechanical properties by hybridizing the surface of AA7075 by hexagonal boron nitride with carbide particles using the FSP process. *J. Mater. Res. Technol.* **2022**, *17*, 1986–1999. [CrossRef]
21. Abushanab, W.S.; Moustafa, E.B.; Melaibari, A.A.; Kotov, A.D.; Mosleh, A.O. A Novel Comparative Study Based on the Economic Feasibility of the Ceramic Nanoparticles Role's in Improving the Properties of the AA5250 Nanocomposites. *Coatings* **2021**, *11*, 977. [CrossRef]
22. Patel, S.K.; Singh, V.P.; Roy, B.S.; Kuriachen, B. Recent research progresses in Al-7075 based in-situ surface composite fabrication through friction stir processing: A review. *Mater. Sci. Eng. B* **2020**, *262*, 114708. [CrossRef]
23. *ASTM E3-11*; Standard Guide for Preparation of Metallographic Specimens 1. ASTM Copyright: West Conshohocken, PA, USA, 2011; Volume i, pp. 1–12. [CrossRef]
24. *ASTM E112-10*; Standard Test Methods for Determining Average Grain Size E112-10. ASTM: West Conshohocken, PA, USA, 2010; Volume 96, pp. 1–27. [CrossRef]
25. Moustafa, E.B.; Taha, M.A. Preparation of high strength graphene reinforced Cu-based nanocomposites via mechanical alloying method: Microstructural, mechanical and electrical properties. *Appl. Phys. A* **2020**, *126*, 220. [CrossRef]
26. Moustafa, E.B.; Elsheikh, A.H.; Taha, M.A. The effect of TaC and NbC hybrid and mono-nanoparticles on AA2024 nanocomposites: Microstructure, strengthening, and artificial aging. *Nanotechnol. Rev.* **2022**, *11*, 2513–2525. [CrossRef]
27. Alsoruji, G.; Moustafa, E.B.; Alzahrani, M.A.; Taha, M.A. Preparation of Silicon Bronze-Based Hybrid Nanocomposites with Excellent Mechanical, Electrical, and Wear Properties by Adding the Ti3AlC2 MAX Phase and Granite Via Powder Metallurgy. *Silicon* **2022**. [CrossRef]
28. Ramadan, S.; Taha, M.A.; El-Meligy, W.M.; Saudi, H.A.; Zawrah, M.F. Influence of Graphene Content on Sinterability and Physico-Mechanical Characteristics of Al/Graphene Composites Prepared via Powder Metallurgy. *Biointerface Res. Appl. Chem.* **2022**, *13*, 192. [CrossRef]
29. Hossein-Zadeh, M.; Razavi, M.; Mirzaee, O.; Ghaderi, R. Characterization of properties of Al–Al2O3 nano-composite synthesized via milling and subsequent casting. *J. King Saud. Univ. Eng. Sci.* **2013**, *25*, 75–80. [CrossRef]
30. Moustafa, E.B.; Alazwari, M.A.; Abushanab, W.S.; Ghandourah, E.I.; Mosleh, A.O.; Ahmed, H.M.; Taha, M.A. Influence of Friction Stir Process on the Physical, Microstructural, Corrosive, and Electrical Properties of an Al–Mg Alloy Modified with Ti–B Additives. *Materials* **2022**, *15*, 835. [CrossRef]
31. AbuShanab, W.S.; Moustafa, E.B.; Ghandourah, E.; Taha, M.A. Effect of graphene nanoparticles on the physical and mechanical properties of the Al2024-graphene nanocomposites fabricated by powder metallurgy. *Results Phys.* **2020**, *19*, 103343. [CrossRef]
32. Hwang, J.; Tak, W.-S.; Mun, S.Y.; Nam, S.; Moon, S.Y.; Kim, W.S. Graphene Encapsulated Al Particles for Improvement of Thermal Conductivity in Composites. *Materials* **2020**, *13*, 3602. [CrossRef]
33. Pradhan, S.K.; Sahoo, M.R.; Ratha, S.; Polai, B.; Mitra, A.; Sathpathy, B.; Sahu, A.; Kar, S.; Satyam, P.V.; Ajayan, P.M.; et al. Graphene-incorporated aluminum with enhanced thermal and mechanical properties for solar heat collectors. *AIP Adv.* **2020**, *10*, 065016. [CrossRef]
34. Sang, M.; Shin, J.; Kim, K.; Yu, K. Electronic and Thermal Properties of Graphene and Recent Advances in Graphene Based Electronics Applications. *Nanomaterials* **2019**, *9*, 374. [CrossRef] [PubMed]

35. AbuShanab, W.S.; Moustafa, E.B.; Ghandourah, E.; Taha, M.A. The Effect of Different Fly Ash and Vanadium Carbide Contents on the Various Properties of Hypereutectic Al-Si Alloys-Based Hybrid Nanocomposites. *Silicon* **2022**, *14*, 5367–5377. [CrossRef]
36. Zhou, W.; Qi, S.; An, Q.; Zhao, H.; Liu, N. Thermal conductivity of boron nitride reinforced polyethylene composites. *Mater. Res. Bull.* **2007**, *42*, 1863–1873. [CrossRef]

Disclaimer/Publisher's Note: The statements, opinions and data contained in all publications are solely those of the individual author(s) and contributor(s) and not of MDPI and/or the editor(s). MDPI and/or the editor(s) disclaim responsibility for any injury to people or property resulting from any ideas, methods, instructions or products referred to in the content.